

## THE INFLUENCE OF PLATING WITH FLAT BARS AROUND TECHNOLOGICAL CUTOUTS ON THE STRESS STATE OF A 37500 TDW CHEMICAL TANKER

**Ana-Maria TARABUSI**

"Dunarea de Jos" University of Galati,  
Faculty of Naval Architecture, Galati, Domneasca  
Street, No. 47, 800008, Romania,  
E-mail: [ana.maria.tarabusi@gmail.com](mailto:ana.maria.tarabusi@gmail.com)

**Anisoara - Gabriela CRISTEA**

"Dunarea de Jos" University of Galati,  
Faculty of Naval Architecture, Galati, Domneasca  
Street, No. 47, 800008, Romania,  
E-mail: [anisoara.cristea@ugal.ro](mailto:anisoara.cristea@ugal.ro)

### ABSTRACT

*The purpose of this study is to determine the stress states of the plating around the technological cutouts of a 37500 tdw chemical tanker under normal operational conditions, taking into account the efficiency of operational optimization and structural strength increase.*

*This study will assess the stress state in the double bottom region of the ship, which experiences the most significant external loads from hydrostatic water pressure and internal loads from cargo pressure.*

**Keywords:** finite element method, hydrostatic water pressure, mechanical structural, stress calculation.

### 1. GENERATION AND ANALYSIS OF THE FE MODEL

The structural analysis was conducted using FEAP/NX Nastran. This software allows the analysis of thermal or structural models with varying degrees of complexity.

The study examined the stress conditions in the ship's double-bottom region under static load conditions in calm water. This was achieved by contrasting two structural configurations: the plated structure and the unplated structure of the vessel.

As such, for both structural variants, comparisons will be made based on the type of finite element used (triangular or quadrilateral) and its size (200 mm, 100 mm, 50 mm) with the scope of observing the influence of flat bars reinforcements around technological cutouts of the stress model.

Additionally, the evolution of stresses will be monitored in 4 distinct ship elements

located on the outline of the cutouts of both the plated and un-plated structures.

The structure itself was modeled using FEMAP, with the vessel dimensions shown in Table 1.1, based on the structural elements that make up the midship section, generated using the POSEIDON ND v.21.4 program package owned by the DNVGL classification company.

**Table 1.1** Dimensions and characteristics of the simplified structure

$L_{pp}=179,960$ [m]	$a_L=0,800$ [m]	El size= 100mm
$B=32,2$ [m]	$a_F=3,200$ [m]	No.ND=192291
$D=16,5$ [m]	$L_{msg}=25,60$ [m]	No. EL=196540

where:

$L_{pp}$  – length between perpendiculars;

$B$  – breadth;

$D$  – depth;

$a_L$  – intercostal distance;

$a_F$  – distance between two floors.

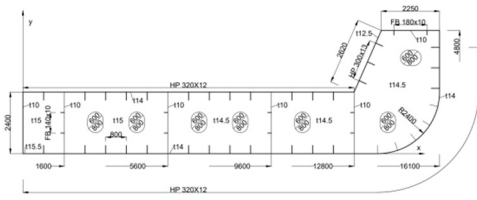


**Fig. 1.1** Simplification and standardization of the CAD structure

## 2. MATERIAL CHARACTERISTICS

The materials used for the generation and analysis must satisfy the criteria for structural integrity, corrosion resistance, long-term durability, and other attributes relevant to the ship and its intended use while also adhering to the standards and regulations set forth by classification societies.

The primary material used in this analysis is high tensile steel with the following characteristics:

- ✓ Yield strength:  $\sigma_c=315$  MPa;
- ✓ Tensile strength:  $\sigma_t = 440$  MPa;
- ✓ Longitudinal elastic modulus:  $E=2,1 \cdot 10^5$  MPa;
- ✓ Poisson's ratio coefficient:  $\nu = 0,3$ ;
- ✓ Material density:  $\rho= 7800$  kg/m<sup>3</sup>.

## 3. GEOMETRY AND MESH

Based on the 3D-CAD model, a 3D-FE model (Figure 1.3a) was generated using the plate and membrane elements of the FE program, and stress concentrations in all structural elements was determined. To highlight stress concentration in all structural elements, it is necessary to use the membrane and plating elements implemented in the FE program.

The FE model utilized the Mindlin Plate theory when representing the physical behavior of plates, with the most common elements used being quadrilaterals, with triangles as the substitute elements where quadrilaterals are not applicable.

Variation in FE elements occurred due to the variation in sizes of the longitudinal profiles and their positions.

To analyze the strength of the ship's hull, the central area of the cargo compartments will be modeled, as it is the most heavily stressed area.

In this study, a 3D structure was modeled along the length of a cargo hold of 25600 mm located in the double-bottom area between frames FR111 and FR143 (Fig. 1.2)

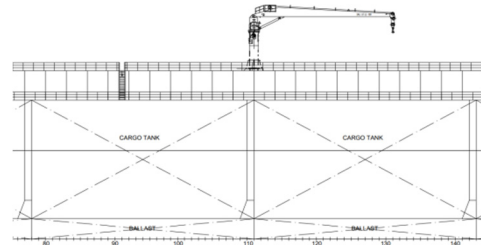


**Fig. 1.2** The central region of the ship

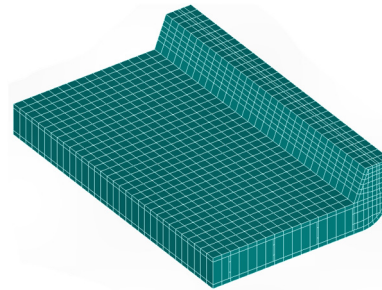


**Fig.1.3a** The extended 3D-CAD structure along the length of a cargo holds of 25600 mm

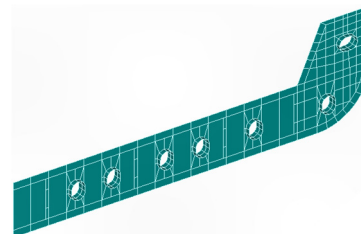


**Fig.1.3b** Plating with flat bars around the technological cutouts

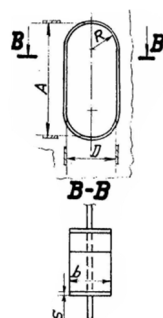


**Fig.1.3c** Geometric characteristics of the plated cutouts

In the case of the plated structure, an additional step is added: plating with flat bars around the cutouts (**Fig. 1.3c**).

In **Fig. 1.3c**, the following geometric characteristics are presented:

- A - the height of the technological cutout (**A = 800 mm**);
- R - the radius of the cutout (**R = 300 mm**);
- D - the diameter of the cutout (**D = 600 mm**);
- B - the width of the flat bar (**b = 200 mm**);
- s - the thickness of the flat bar (**s = t** - the thickness of the web of the flange).

During production, the flat bar can be made either from a single piece or from two pieces of bar stock, joined together as shown in section B-B.

Also, following the making of the 3D-FE model, 192291 nodes and 196540 elements resulted (**Fig. 1.4a** and **Fig. 1.4b**).

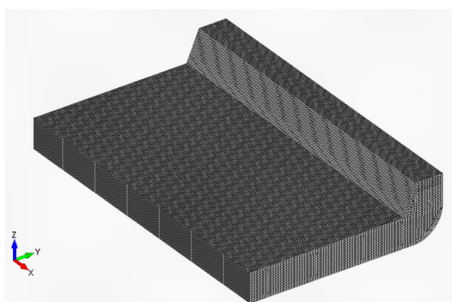


**Fig.1.4a** The complete 3D-FE model of the double-bottom structure

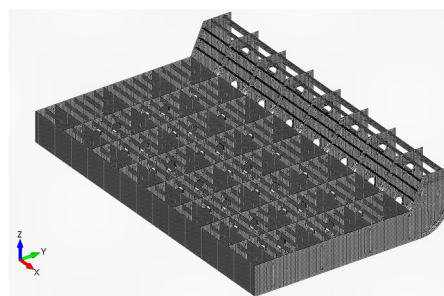


**Fig.1.4b** Highlighting the 3D-FE structural elements

The table below presents the types of discretization elements employed as well as the dimensions of the FE structure:

**Table 1.2** Characteristics of the used elements

The type of structure	The type of element	The dimension of the element	Nr. of nodes	Nr. of elements
Unplated	QUAD	50 mm	794687	800672
		100 mm	192291	196540
		200 mm	52790	54778
	TRI	50 mm	791487	159632
		100 mm	196394	399548
		200 mm	52897	109333
Plated	QUAD	50 mm	814021	819488
		100 mm	196211	200460
		200 mm	53770	55758
	TRI	50 mm	810989	1615348
		100 mm	200489	403468
		200 mm	53877	110313

#### 4. EDGE CONDITIONS

Boundary conditions refer to the requirements applied to the geometric boundaries of a model to subject it to real world loading conditions and obtain a relevant result. (Figure 1.5).

The edge conditions applied to the FE model have the role of simulating the existence of real structures in the aft, fore and bilge region of the vessel.

The edge conditions used for the study of the model are shown in **Table 1.3**.

**Table 1.3** Boundary conditions for the 3D - FE model

Boundary condition	Blocked degrees of freedom					
	T <sub>x</sub>	T <sub>y</sub>	T <sub>z</sub>	R <sub>x</sub>	R <sub>y</sub>	R <sub>z</sub>
Symmetry in the diametral plane PD	-	x	-	x	-	x
The condition at the level of stringers	-	-	x	-	-	-
The condition of symmetry with respect to the adjacent cargo hold in the aft (PP)	x	x	x	x	-	x
The condition of symmetry with respect to the adjacent cargo hold in the bow (PV)	-	x	x	x	-	x

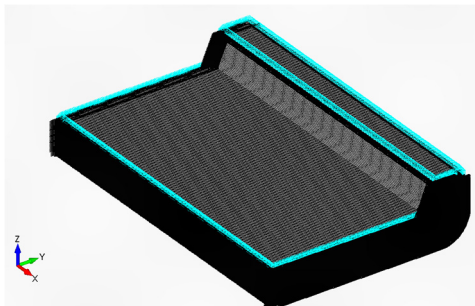


**Fig. 1.5** Boundary conditions for the 3D - FE model

## 5. LOADS APPLIED UPON THE MODEL

### The case of static placement on still water

The FE model is subjected to the following types of loads:

- Gravitational load given by the net weight of the structural elements of the vessel:  $g = 9.81 \text{ m/s}^2$ ,  $\rho = 7.8 \text{ t/m}^3$  and other components on board of the vessel around the modeled cargo tank.

- The Cargo load, idealized on the double bottom shell, double hull, longitudinal and transversal walls, as hydrostatic pressure of the cargo ( $\rho = 1.05 \text{ t/m}^3$ ) [N/mm<sup>2</sup>], for a reference quota HHC (D=14100 mm).

The hydrostatic pressure equation used is given in (1):

$$p = \rho g z \text{ [kN/m}^2\text{]} \quad (1)$$

where:

- $\rho$  – density of transported goods [t/m<sup>3</sup>];
- $g$  – gravitational acceleration [m/s<sup>2</sup>];
- $z$  – vertical distance to the highest point the goods reach inside the warehouse [m].

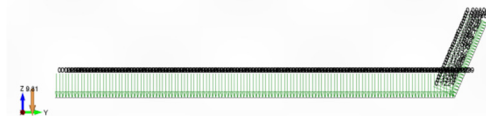


**Fig. 1.6** Hydrostatic cargo pressure distribution ( $\rho_{\text{cargo}} = 1.05 \text{ t/m}^3$ )

- Still water load:

The Still water load results immersion of the vessel hull in seawater. It is idealized on the outer shell, as the hydrostatic pressure in the seawater ( $\rho = 1,025 \text{ t/m}^3$ ), for a full load draught of  $T = 14500 \text{ mm}$  (Fig. 1.7).

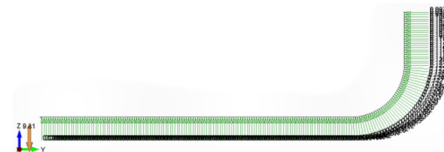


**Fig. 1.7** Hydrostatic pressure generated by the still water ( $\rho_{\text{water}} = 1,025 \text{ t/m}^3$ )

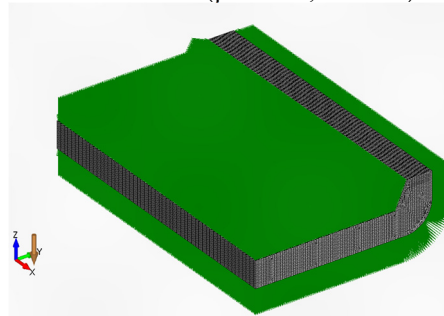


**Fig. 1.8** The loads applied to the 3D-FE model on the inner and outer shell

## 6. FE ANALYSIS RESULTS

### A. Stresses and deformations of the un-plated structure for an average discretization of 100 mm

Regarding the tensions in the unbound 3D-FE structures, with the help of the following figures, we observed that:

- ✓ On the framed 3D-FE structure, the Von Mises stresses have a maximum value of 250.68 MPa in the bottom longitudinal area.
- ✓ On the reinforced flanges, the Von Mises stresses reach a maximum value of 171.30 MPa.
- ✓ On the sealed flanges, the stresses decrease, reaching a maximum value of 78.704 MPa.
- ✓ The Von Mises stresses in the supports and the Bilge stringer reached a maximum value of 85.08 MPa.
- ✓ On the double bottom's ceiling and the inclined ceiling of the bilge tank, the stresses reached a maximum value of 146.41 MPa.

On the bottom and the bilge shell, they have a maximum value of 197.8 MPa.

All these Von Mises stresses do not exceed the maximum allowable stress of the steel utilized.

Additionally, regarding deformations in the unbounded 3D-FE model, it can be observed that:

- ✓ On the framed 3D-FE model, displacements are significant in the central area of the cargo hold around the Center Plane, with maximum deformations reaching a value of 10.22 mm.
- ✓ The displacements that occurred in the reinforcement flanges have a maximum value of 5.01 mm.
- ✓ In the case of the sealed flanges, the displacements were small, with a maximum value of 1.52 mm.
- ✓ The displacements in the longitudinal supports and the Bilge stringers have a maximum value of 4.95 mm.

✓ In the bottom longitudinal, double bottom, and bilge, the deformation reached a maximum value of 7.02 mm.

✓ The displacements that occurred in the double bottom ceiling and the inclined ceiling of the bilge tank reached a maximum value of 5.88 mm.

The bottom and bilge shell reached a record maximum deformations of 10.22 mm.

For the interpretation of the analysis, the maximum stresses in the structure and the medium stresses on the elements will be considered (**Fig. 1.9** and **Fig. 1.10**).

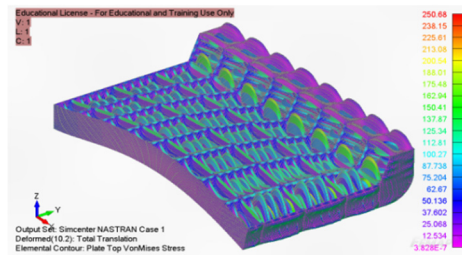


**Fig. 1.1** In the case of calm water, Von Mises stresses on the complete 3D-FE model.

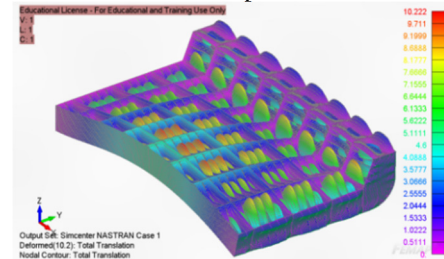


**Fig. 1.10** In the case of calm water, the displacements (complete 3D-FE model)

### B. Stresses and deformations of the framed structure for an average discretization of 100 mm.

Regarding the stresses in the framed 3D-FE structure, with the help of the following figures (**Fig. 1.11**), we noticed that:

- ✓ On the reinforced flanges, the Von Mises stresses reached a maximum value of 177.74 MPa.
- ✓ On the framed 3D-FE structure, the Von Mises stresses had a maximum value of 250.86 MPa in the bottom longitudinal area.



- ✓ On the framed 3D-FE structure, the Von Mises stresses had a maximum value of 250.86 MPa in the bottom longitudinal area.
- ✓ On the sealed flanges, the stresses decreased, reaching a maximum value of 78.699 MPa.
- ✓ The Von Mises stresses in the supports and the bilge's stringer have a maximum value of 86.08 MPa.
- ✓ On the double bottom's ceiling and the inclined ceiling of the bilge tank, the stresses reach a maximum value of 146.4 MPa.
- ✓ On the bottom and bilge shell, they had a maximum value of 197.8 MPa.

All these Von Mises stresses did not exceed the maximum allowable stress of the steel used.

Furthermore, in the case of deformations in the framed 3D-FE structure, we observed (Fig. 1.12):

- ✓ On the framed 3D-FE structure, displacements were significant in the central area of the cargo hold around the Central Plane, with a maximum deformation value of 10.16 mm.
- ✓ The displacements that occurred in the reinforced flanges had a maximum value of 4.98 mm.
- ✓ In the case of the sealed flanges, displacements were small with a maximum value of 1.51 mm.
- ✓ The displacements in the supports and the bilge stringers had a maximum value of 4.91 mm.
- ✓ In the bottom longitudinals, double bottom, and bilge, the deformations reached a maximum value of 6.96 mm.
- ✓ The displacements that occurred in the double bottom ceiling and the inclined ceiling of the bilge tank reached a maximum value of 5.87 mm.
- ✓ The bottom and the bilge shell recorded a maximum deformation of 10.16 mm.

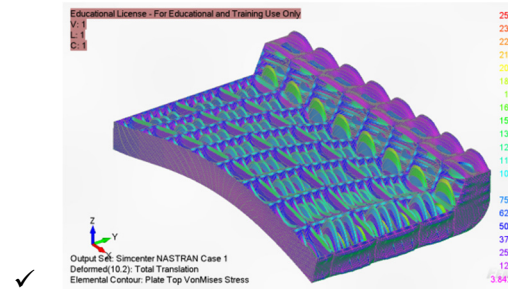


Fig. 1.11 In the case of calm water conditions, Von Mises stresses (3D-FE model)

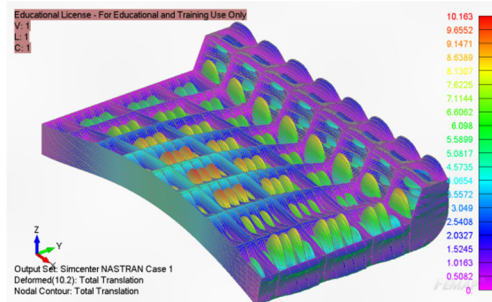


Fig. 1.12 In the case of calm water conditions, the displacements (3D-FE model)

### C. VARIATIONS IN STRESSES AROUND CUTOUTS.

To analyze stress variations around cutouts, four symmetrically positioned zones have been chosen, located around the circumference of the cutout, for both the framed and unframed FE models (Fig. 1.13).

To achieve the most precise result, it was necessary to analyze the 3D-FE structure through variations with increasingly finer discretization, starting from 200 mm (coarse discretization), moving to 100 mm (medium discretization), and eventually reaching 50 mm (fine discretization).

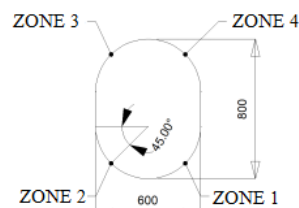


Fig. 1.13 Detail of the areas of analyzed elements around the cutouts.

**MESH QUAD – UNPLATED STRUCTURE**

Stress variations of the elements  
(MESH QUAD 200 mm)

ID	VonMises Stress (MPa)
Zone 1	42.683
Zone 2	34.888
Zone 3	34.293
Zone 4	35.076

Stress variations of the elements  
(MESH QUAD 100 mm)

ID	VonMises Stress (MPa)
Zone 1	43.606
Zone 2	35.565
Zone 3	34.508
Zone 4	35.027

Stress variations of the elements  
(MESH QUAD 50 mm)

ID	VonMises Stress (MPa)
Zone 1	54.752
Zone 2	46.127
Zone 3	44.000
Zone 4	42.955

**MESH QUAD – PLATED STRUCTURE**

Stress variations of the elements  
MESH QUAD 200 mm

ID	VonMises Stress (MPa)
Zone 1	39.034
Zone 2	33.017
Zone 3	32.086
Zone 4	34.370

Stress variations of the elements  
(MESH QUAD 100 mm)

ID	VonMises Stress (MPa)
Zone 1	39.909
Zone 2	33.491
Zone 3	32.692
Zone 4	33.019

Stress variations of the elements  
(MESH QUAD 50 mm)

ID	VonMises Stress (MPa)
Zone 1	48.213
Zone 2	40.906
Zone 3	43.490
Zone 4	37.111

**MESH TRI - UNPLATED STRUCTURE**

Stress variations of the elements  
MESH TRI 200 mm

ID	VonMises Stress (MPa)
Zone 1	62.365
Zone 2	51.931
Zone 3	52.529
Zone 4	51.639

Stress variations of the elements  
MESH TRI 100 mm

ID	VonMises Stress (MPa)
Zone 1	54.087
Zone 2	61.588
Zone 3	44.334
Zone 4	59.834

Stress variations of the elements  
MESH TRI 50 mm

ID	VonMises Stress (MPa)
Zone 1	71.188
Zone 2	56.629
Zone 3	58.529
Zone 4	55.867

**MESH TRI - PLATED STRUCTURE**

Stress variations of the elements  
MESH TRI 200 mm

ID	VonMises Stress (MPa)
Zone 1	44.448
Zone 2	37.700
Zone 3	38.347
Zone 4	41.610

Stress variations of the elements  
MESH TRI 100 mm

ID	VonMises Stress (MPa)
Zone 1	47.471
Zone 2	47.117
Zone 3	40.889
Zone 4	49.592

Stress variations of the elements  
MESH TRI 50 mm

ID	VonMises Stress (MPa)
Zone 1	55.722
Zone 2	46.664
Zone 3	47.284
Zone 4	45.396

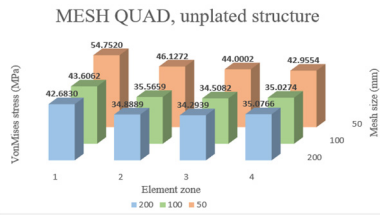


Fig. 1.14 Stress variations of the elements for a quad mesh (unplated structure B-)

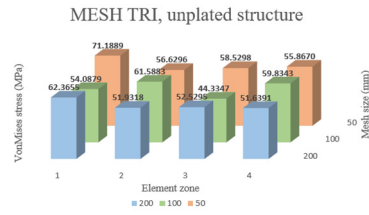


Fig. 1.16 Stress variations of the elements for a tri mesh (unplated structure B+)

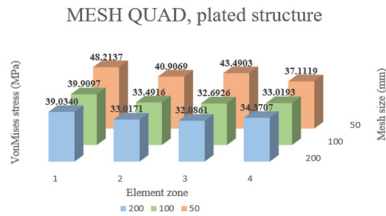


Fig. 1.15 Stress variations of the elements for a quad mesh (plated structure B+)

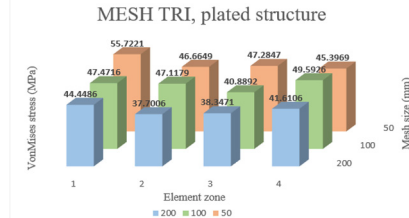


Fig. 1.17 Stress variations of the elements for a tri mesh (plated structure B+)

The percentage differences between the values obtained for a quad mesh:

a) MESH QUAD 200 mm

ZONE	B-	B+	(%)
1	42.6830	39.0340	8.5491
2	34.8889	33.0171	5.3650
3	34.2939	32.0861	6.4379
4	35.0766	34.3707	2.0124

b) MESH QUAD 100 mm

ZONE	B-	B+	(%)
1	43.6062	39.9097	8.4771
2	35.5659	33.4916	5.8323
3	34.5082	32.6926	5.2615
4	35.0274	33.0193	5.7329

c) MESH QUAD 50 mm

ZONE	B-	B+	(%)
1	54.7520	48.2137	11.9417
2	46.1272	40.9069	11.3171
3	44.0002	43.4903	1.1589
4	42.9554	37.1119	13.6037

The percentage differences between the values obtained for a tri mesh:

a) MESH TRI 200 mm

ZONE	B-	B+	(%)
1	62.3655	44.4486	28.7288
2	51.9318	37.7006	27.4036
3	52.5295	38.3471	26.9990
4	51.6391	41.6106	19.4203

b) MESH TRI 100 mm

ZONE	B-	B+	(%)
1	63.5883	47.4716	12.2325
2	61.5883	47.1179	23.4953
3	44.3347	40.8892	7.7716
4	59.8343	49.5926	17.1168

c) MESH TRI 50 mm

ZONE	B-	B+	(%)
1	71.1889	55.7221	21.7265
2	56.6296	46.6649	17.5963
3	58.5298	47.2847	19.2126
4	55.8670	45.3969	18.7411



Additionally, the type of element influenced the obtained values, which is why both quad and triangular finite elements were used.

The completion of this step was based on selecting a reinforced stringer of the 3D-FE model for all types of discretization and studying the stress state behavior in the absence and presence of plating with flat bars around technological cutouts.

In the following figures, the differences between these cases are presented, and it was observed that:

- ✓ The Von Mises stresses on the reinforced stringers in the unplated 3D-FE structure formed stress concentrations around the cutouts.
- ✓ The Von Mises stresses on the reinforced stringers in the plated 3D-FE structure decreased, avoiding the formation of stress concentrations around these cutouts.
- ✓ The values of Von Mises stresses increased if other structural elements such as longitudinal profiles were present near the cutouts and if another cutout is present in the close vicinity.
- ✓ The lower area of the bilge is the least affected by stress state influence. Finer discretization led to higher VonMises stress values.

Zone 1 on the circumference of the cutout was the most affected area, with the highest values.

## 7. CONCLUSIONS

From a global perspective, the process of plating with flat bars around the cutouts of a 3D-FE model in the double-bottom region of a chemical tanker has the following effects:

- ✓ Reduction of Von Mises stresses;
- ✓ Reduction of structural deformations.

From a local perspective, analysis of the influence of plating with flat bar reinforcements around a specific cutout of a stringer, showed that:

- ✓ The effect of the plating process contributes to reducing stresses and deformations in the ship's structure by standardizing the distribution of external loads and preventing the occurrence of stress concentrations that could affect structural strength.
- ✓ The presence of structural elements in the vicinity of the cutout influences the stress state around the cutout.
- ✓ The presence of other cutouts around the analyzed cutout also influences the stress state around the cutout.
- ✓ The lower part of the cutout with most stress concentrations.

The flat bar reinforcement used for plating absorbs some of the loads around the cutout.

This calculation method can be successfully used to analyze the variation of stresses in the double-bottom area of the ship.

## 8. REFERENCES

- [1] Cook, R. D., *Finite Element Modeling for Stress Analysis*, Wiley, New York, 1995.
- [2] Cristea A.G., *Contribuții privind optimizarea structurilor de navă*, Teză de doctorat, Galați, 2014
- [3] Jonathan Whiteley, *Finite Element Methods*, Ed. Springer International Publishing AG, 2007
- [4] Moguș C., Cristea A-G, *Determination of stress state and deformations that can appear in transversal frames of a 48309 dwt bulk carrier*, The Annals of "Dunarea de Jos" University of Galati, 2023
- [5] x x x – Siemens PLM Software Inc., „FNN, Femap/NX Nastran users' manual,” 2020
- [6] x x x – DNV, Poseidon User Manual, v.21.4

- [7] x x x – DNV rules for classification, Ships (RU-SHIP), <https://www.dnvgl.com/rules-standards/>  
x x x – <http://www.iacs.org.uk/publications/common-structural-rules/csr-for-bulk-carriers-and-oil-tankers/>
- [8]

- [9] x x x – FEAP 12.0.1a / NX NASTRAN User's Guide, UGS Corporation / Siemens PLM Software Inc., 2021

*Paper received on November 6<sup>th</sup> 2023*